

See discussions, stats, and author profiles for this publication at: <https://www.researchgate.net/publication/229520713>

# Controlled Radical Polymerization of Vinyl Acetate Mediated by a Bis(imino)pyridine Vanadium Complex

ARTICLE in *MACROMOLECULES* · DECEMBER 2011

Impact Factor: 5.8 · DOI: 10.1021/ma200734g

CITATIONS

19

READS

55

9 AUTHORS, INCLUDING:



**Michael Jones**

Simon Fraser University

8 PUBLICATIONS 96 CITATIONS

SEE PROFILE



**Jason K Pearson**

University of Prince Edward Island

28 PUBLICATIONS 240 CITATIONS

SEE PROFILE



**Tim Storr**

Simon Fraser University

60 PUBLICATIONS 1,402 CITATIONS

SEE PROFILE



**Michael Shaver**

The University of Edinburgh

61 PUBLICATIONS 888 CITATIONS

SEE PROFILE

# Controlled Radical Polymerization of Vinyl Acetate Mediated by a Bis(imino)pyridine Vanadium Complex

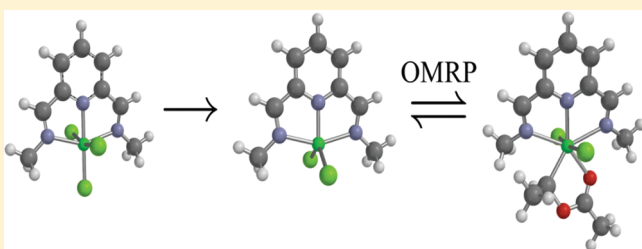
Laura E. N. Allan,<sup>†</sup> Edward D. Cross,<sup>†</sup> Timothy W. Francis-Pranger,<sup>†</sup> M. Emre Hanhan,<sup>†</sup> Michael R. Jones,<sup>‡</sup> Jason K. Pearson,<sup>†</sup> Mitchell R. Perry,<sup>†</sup> Tim Storr,<sup>‡</sup> and Michael P. Shaver<sup>\*,†</sup>

<sup>†</sup>Department of Chemistry, University of Prince Edward Island, 550 University Avenue, Charlottetown, PE C1A 4P3, Canada

<sup>‡</sup>Department of Chemistry, Simon Fraser University, 8888 University Drive, Burnaby, BC V5A 1S6, Canada

## S Supporting Information

**ABSTRACT:** The mechanism of controlled radical polymerization of vinyl acetate using vanadium catalysts is investigated using a range of experimental and computational studies. Optimal control is achieved using the noninnocent bis(imino)pyridine ligand framework. [BIMPY]VCl<sub>3</sub>, where BIMPY = 2,6-[(2,6-*i*-Pr<sub>2</sub>C<sub>6</sub>H<sub>3</sub>)N=C(Me)]<sub>2</sub>(C<sub>5</sub>H<sub>3</sub>N)), is one of only a few transition metal systems capable of mediating the polymerization of vinyl acetate. Initiation using AIBN at 120 °C results in excellent control over poly(vinyl acetate) molecular weights and PDIs to give vanadium-terminated polymer chains which can be readily converted to both proton-terminated poly(vinyl acetate) or poly(vinyl alcohol). Irreversible halogen transfer from the parent [BIMPY]VCl<sub>3</sub> complex to a radical derived from AIBN generates the active species, [BIMPY]VCl<sub>2</sub>. This catalyst cannot use the halogen atom transfer equilibrium to control polymerization but can act as a persistent radical and trap the propagating polymer chains through an OMRP reversible termination process. Computational studies support this novel two-step reaction pathway and reveal that the poor control exerted over styrene versus the excellent control observed for vinyl acetate under these conditions is not only dependent on radical reactivity but also due to chelation of the carbonyl group of vinyl acetate to the vanadium center, making the trapping step more favorable. This correlates with an energy difference of just 4 kcal/mol between the reduced [BIMPY]VCl<sub>2</sub>, and [BIMPY]VCl<sub>2</sub>R species for vinyl acetate compared to over 20 kcal/mol for styrene. This [BIMPY]VCl<sub>3</sub> system can be extended to other vinyl ester monomers, with good control over molecular weights and PDIs obtained for vinyl propionate, vinyl pivalate, and vinyl benzoate.



## INTRODUCTION

Radical polymerization occupies an important position in commercial polymer production because of the scope of applicable monomers, the functional group tolerance, the wide range of reaction conditions, and the lower relative infrastructure costs. Unfortunately, these conventional reactions have significant limitations with respect to a chemist's ability to control the molecular weight distribution, molecular architecture, and composition of the polymers. In order to exact this control, several methodologies have been developed which reduce radical concentrations and efficiently exchange dormant chains with reactive radical species in order to minimize bimolecular termination reactions. The nature of the dormant chain differentiates these processes, with nitroxide-mediated radical polymerization (NMP)<sup>1,2</sup> exploiting the reversible cleavage of a nitroxide-carbon bond, thiocarbamates supporting a reversible addition-fragmentation chain transfer (RAFT)<sup>2,3</sup> pathway, and ruthenium and copper complexes mediating the exchange of halogen-capped polymer chains through an atom transfer radical polymerization (ATRP).<sup>4,5</sup> Together these processes are termed controlled radical polymerization (CRP) and provide extraordinary control over polymer molecular weight and molecular weight distributions.

Great interest has been placed on the development of CRP mediated by transition metals due to the inherent tunability of metal complexes through alteration of the ligand framework and the flexibility of metal oxidation states in supporting one-electron transformations.<sup>6,7</sup> While ATRP dominates metal-mediated radical polymerization, organometallic-mediated radical polymerization (OMRP) is experiencing significant growth.<sup>8</sup> OMRP involves trapping radicals through the formation of a metal-carbon bond to generate an organometallic species. It requires a metal center with a reversible one-electron redox couple and metal-carbon bonds weak enough to be homolytically cleaved under reaction conditions. Waymouth first developed Co-porphyrin complexes for the OMRP of acrylates in 1994.<sup>9</sup> Recently, cobalt-mediated radical polymerizations have been expanded to vinyl acetate using a bis(acetylacetonato)cobalt(II) complex.<sup>10</sup> These systems function optimally when a low-temperature radical initiator, 2,2'-azobis(4-methoxy-2,4-dimethylvaleronitrile), is used to establish a degenerative transfer mechanism to exchange growing

Received: March 30, 2011

Revised: April 26, 2011

Published: May 05, 2011

radical chains. In the presence of electron donors such as water or pyridine this system operates via reversible termination OMRP, also exerting excellent control over vinyl acetate polymerization.<sup>11–13</sup> While OMRP mechanisms have also been implied for molybdenum,<sup>14–16</sup> osmium,<sup>17</sup> iron,<sup>18,19</sup> and chromium<sup>20–22</sup> complexes, these systems do not afford effective control.

The CRP of vinyl acetate is of particular interest because this monomer can only be polymerized through radical mechanisms, the polymers are readily hydrolyzed to form biodegradable poly(vinyl alcohol)s, and there remains a paucity of systems capable of controlling this reaction due to the relatively high reactivity of the propagating radical species and the strong bonds these radicals can form with traditional trapping end-groups. While sulfur-based degenerative transfer methods have been reported,<sup>23–25</sup> OMRP affords the best level of control, with the aforementioned cobalt system producing polymers with polydispersity indices as low as 1.1.<sup>10,11,26</sup> This system is not operationally ideal, however, as it depends upon a thermally unstable azo radical source which must be stored at  $-20\text{ }^{\circ}\text{C}$  and employs polymerization temperatures of  $30\text{ }^{\circ}\text{C}$ . As the radical polymerization process is exothermic, maintaining low temperatures on industrial scales is a significant challenge, although cobalt-containing macroinitiators have provided improved control in laboratory scale reactions.<sup>26</sup> It is clear that further research is necessary; to both expand the range of complexes and the operational conditions for the CRP of vinyl acetate.

We recently reported our preliminary results on a novel vanadium-mediated radical polymerization where [BIMPY]- $\text{VCl}_3$ , **1**, was effective for the CRP of vinyl acetate at  $120\text{ }^{\circ}\text{C}$ .<sup>27</sup> Herein we expand on these results and present a more detailed picture of the role of the complex in controlling this important polymerization. We include a computational analysis of a number of potential reaction pathways for this controlled radical polymerization, an expansion of the polymerization scope, and details of the electronic nature of the parent complex **1**. The system operates at industrially relevant temperatures through a mechanism unique to CRP and shows great promise in the preparation of vinyl ester macromolecular structures.

## ■ EXPERIMENTAL SECTION

**Materials.** HPLC-grade dichloromethane, acetonitrile, toluene, chloroform, and tetrahydrofuran were purchased from Fisher Scientific, while deuterated solvents were purchased from Cambridge Isotopes. Acetonitrile and dichloromethane were dried by refluxing over calcium hydride for 48 h, distilling under a dinitrogen atmosphere and thoroughly degassing the solvent. Anhydrous toluene, THF, pentane, and diethyl ether were obtained by passing the solvent through an Innovative Technologies solvent purification system consisting of columns of alumina and a copper catalyst. Anhydrous solvents were tested with addition of a toluene solution of sodium benzophenone ketyl and were degassed prior to use. Deuterated solvents were dried by refluxing over an appropriate drying agent for 48 h and then trap-to-trap distilled and freeze–pump–thaw degassed three times. Monomers styrene, methyl methacrylate, acrylonitrile, vinyl acetate, vinyl pivalate, vinyl propionate, and vinyl benzoate, purchased from Aldrich Chemical Co., were dried by stirring over calcium hydride for 24 h and were then vacuum transferred or distilled and degassed prior to use. Azobis(isobutyronitrile), AIBN, was recrystallized from methanol prior to use. All other chemicals were purchased from Aldrich Chemical Co.; solid reagents were used as received while liquids were distilled under nitrogen before use.  $\text{VCl}_3(\text{THF})_3$ ,<sup>28</sup>  $\text{VCl}_2(\text{py})_4$ ,<sup>29</sup>  $\text{VCl}_2(\text{TMEDA})_2$ ,<sup>30</sup>  $[\text{V}_2(\mu\text{-Cl})_3(\text{THF})_6]_2[\text{Zn}_2\text{Cl}_6]$ ,<sup>30</sup> and the

bis(imino)pyridine proligand BIMPY<sup>31</sup> ( $\text{BIMPY} = 2,6\text{-}[(2,6\text{-iPr}_2\text{C}_6\text{H}_3)\text{-N}=\text{C}(\text{Me})]_2(\text{C}_5\text{H}_3\text{N})$ ) were prepared according to established literature procedures. The complex  $[\text{BIMPY}]\text{VCl}_3$  was synthesized via a modified literature procedure<sup>32</sup> in  $\text{CH}_2\text{Cl}_2$  and recrystallized from acetonitrile prior to use.

**General Considerations.** All experiments involving moisture- and air-sensitive compounds were performed under a nitrogen atmosphere using an MBraun LABmaster sp glovebox system equipped with a  $-35\text{ }^{\circ}\text{C}$  freezer and  $[\text{H}_2\text{O}]$  and  $[\text{O}_2]$  analyzers or using standard Schlenk techniques. Gel permeation chromatography (GPC) was carried out in THF or  $\text{CHCl}_3$  (flow rate:  $1\text{ mL min}^{-1}$ ) at  $50\text{ }^{\circ}\text{C}$  with a Polymer Laboratories PL-GPC 50 Plus integrated GPC system using three  $300 \times 7.5\text{ mm}$  Resipore columns. Polystyrene standards were used for calibration and corrected for PVAc against parameters for low molecular weight vinyl acetate.<sup>33</sup>  $^1\text{H}$  NMR and 2-D spectra were recorded at  $298\text{ K}$  with a Bruker Avance spectrometer ( $300\text{ MHz}$ ) in  $\text{CD}_3\text{CN}$ ,  $\text{CDCl}_3$ , or  $\text{C}_6\text{D}_6$ . Elemental analyses were conducted by Guelph Analytical Laboratories. Cyclic voltammetry (CV) was performed on a PAR-263A potentiometer, equipped with a Ag wire reference electrode, a platinum disk working electrode, and a Pt counter electrode with either  $0.1\text{ M Bu}_4\text{NClO}_4$  or  $\text{Bu}_4\text{NPF}_6$  solutions in  $\text{CH}_2\text{Cl}_2$  or  $\text{CH}_3\text{CN}$ . Ferrocene was used as an internal standard. EPR spectra were collected using a Bruker EMXplus spectrometer operating with a premiumX X-band ( $9.5\text{ GHz}$ ) microwave bridge. The sample was placed in a quartz capillary for measurements. EPR spectra were simulated with a Bruker WINEPR and Simfonia software package. X-ray photoelectron spectra were obtained using a Kratos Analytical Axis ULTRA spectrometer containing a DLD detector.

**Synthesis of  $[\text{PMDETA}]\text{VCl}_2$  (**2**).** This procedure was modified from the preparation of  $\text{VCl}_2(\text{TMEDA})_2$ .  $[\text{V}_2(\mu\text{-Cl})_3(\text{THF})_6]_2\text{-}[\text{Zn}_2\text{Cl}_6]$  ( $1.25\text{ g}$ ,  $0.8\text{ mmol}$ ) was suspended in  $20\text{ mL}$  of THF under an inert atmosphere. A solution of PMDETA ( $2.66\text{ g}$ ,  $15.3\text{ mmol}$ ) in  $20\text{ mL}$  of THF was added dropwise via an addition funnel. The mixture changed from a deep green to a pale purple over the addition window ( $30\text{ min}$ ) and was then stirred for a further  $24\text{ h}$  at room temperature. A pale purple solid was isolated through filtration, washed with cold THF and pentane, and dried *in vacuo* to afford **2** as an air-sensitive pale blue solid ( $0.45\text{ g}$ ,  $88\%$  yield). The product was characterized by elemental and Evans' NMR analysis. No assignable  $^1\text{H}$  NMR signals were found. Anal. Calcd for  $\text{C}_9\text{H}_{23}\text{N}_3\text{VCl}_2$ : C,  $36.62$ ; H,  $7.85$ ; N,  $14.24$ . Found: C,  $36.28$ ; H,  $7.67$ ; N,  $13.91$ . IR (Nujol mull,  $\text{KBr}$ ,  $\text{cm}^{-1}$ ):  $2359\text{ (w)}$ ,  $1020\text{ (br, w)}$ ,  $799\text{ (w)}$ ,  $668\text{ (w)}$ .  $\mu_{\text{eff}} = 3.68\text{ }\mu_{\text{B}}$ .

**Synthesis of  $[\text{PMDETA}]\text{VCl}_3$  (**6**).**  $\text{VCl}_3(\text{THF})_3$  ( $0.95\text{ g}$ ,  $2.5\text{ mmol}$ ) was dissolved in  $30\text{ mL}$  of THF under an inert atmosphere. PMDETA ( $2.20\text{ g}$ ,  $12.7\text{ mmol}$ ) was added dropwise with vigorous stirring to this red solution, forming a deep purple solution. The solution was stirred for  $6\text{ h}$ , and then the solvent was removed *in vacuo*. The resulting purple solid was washed with cold diethyl ether and pentane and dried extensively to remove the remaining THF and isolate **6** ( $0.38\text{ g}$ ,  $45\%$ ). The product was characterized by  $^1\text{H}$  NMR spectroscopy as well as elemental and Evans' NMR analysis. Anal. Calcd for  $\text{C}_9\text{H}_{23}\text{N}_3\text{VCl}_3$ : C,  $32.70$ ; H,  $7.01$ ; N,  $12.71$ . Found: C,  $33.04$ ; H,  $7.18$ ; N,  $12.95$ .  $\mu_{\text{eff}} = 2.81\text{ }\mu_{\text{B}}$ .  $^1\text{H}$  NMR ( $\delta$ ,  $300\text{ MHz}$ ,  $\text{C}_6\text{D}_6$ ):  $-22.24\text{ (br)}$ ,  $-22.81\text{ (br)}$ ,  $-4.25\text{ (br)}$ ,  $-2.89\text{ (br)}$ ,  $6.36\text{ (br)}$ ,  $8.18\text{ (br)}$ ,  $9.30\text{ (br)}$ .

**General Polymerization Procedures.** Monomer, catalyst, and initiator were placed in an ampule under inert atmosphere. For reactions carried out under ATRP conditions, the ratios used were  $100:1:1$  and the initiator was 1-PECL. For reactions carried out under OMRP and r-ATRP conditions, the ratios were  $100:1:0.6$  and the initiator was AIBN. The ampule was placed in a preheated oil bath for the required length of time, then removed from the heat, and cooled quickly under running water. Workup procedures were dependent on the monomer: poly(styrene), poly(methyl methacrylate), and poly(acrylonitrile) samples were dissolved in  $5\text{ mL}$  of THF and precipitated into  $100\text{ mL}$  of

acidified methanol (1% HCl). Poly(vinyl benzoate) was dissolved in  $\text{CH}_2\text{Cl}_2$  (5 mL) and precipitated into hexanes (100 mL). For poly(vinyl acetate), poly(vinyl propionate), and poly(vinyl pivalate), excess monomer was removed under reduced pressure. All polymer samples were dried to constant mass and then weighed to determine monomer conversion gravimetrically.

**Representative Polymerization Procedure.** BIMPYVCl<sub>3</sub> (0.06 g, 0.1 mmol), AIBN (0.01 g, 0.06 mmol), and vinyl propionate (1.0 g, 10 mmol) were added to an ampule under inert atmosphere, which was then sealed and heated at 120 °C for 6 h. Drying *in vacuo* for 48 h gave 0.21 g of poly(vinyl propionate), corresponding to 20% conversion ( $M_{n,\text{th}} = 3990$ ) with  $M_n = 3529$  and PDI = 1.35.

**Preparation of Proton-Terminated PVAc.** Red, vanadium-capped, poly(vinyl acetate) (0.20 g,  $M_n = 4080$ ) was suspended in 10 mL of degassed methanol under an inert atmosphere. To this mixture was added a molar excess of 1-propanethiol (0.10 g). The resulting red solution was heated to 50 °C for 24 h. The polymer was precipitated by dropwise addition to hexanes before being isolated by filtration and dried *in vacuo*. The resulting off-white polymer (0.12 g,  $M_n = 3077$ ) was analyzed by GPC and <sup>1</sup>H NMR spectroscopy. <sup>1</sup>H NMR ( $\delta$ , 300 MHz,  $\text{CDCl}_3$ ): 4.86 ( $\text{CH}_2\text{CHOCOCH}_3$ , polymer chain), 3.87 ( $\text{CH}_2\text{CH}_2\text{OCOCH}_3$ , proton-terminated chain end), 2.04 ( $\text{CH}_2\text{CHOCOCH}_3$ , polymer chain), 1.7–1.9 ( $\text{CH}_2\text{CHOCOCH}_3$  and  $\text{CH}_2\text{CHOCOCH}_3$ , polymer chain and end); 1.4–1.5 (AIBN, partially obscured). Preparation of higher molecular weight proton-terminated poly(vinyl acetate) chains required longer reaction times (~48 h). For example, 0.10 g of  $M_n = 5750$  PVAc was converted to 0.08 g of  $M_n$  5040 proton-terminated PVAc after 48 h of treatment with 1-propanethiol.

**Hydrolysis of PVAc.** Poly(vinyl acetate) was converted into the corresponding poly(vinyl alcohol) by base-catalyzed methanolysis. A solution of vanadium end-capped PVAc (0.20 g,  $M_n = 4900$ ) dissolved in 5 mL of THF was added dropwise to a solution of KOH (0.05 g) in 10 mL of methanol. After stirring this mixture for 48 h at room temperature, the solvent was removed *in vacuo*, and the residue dissolved in distilled water and precipitated by addition to 10 mL of cold acetone. The product was collected by filtration, dried, and analyzed by <sup>1</sup>H NMR spectroscopy, producing a white, water-soluble polymer (0.12 g). <sup>1</sup>H NMR ( $\delta$ , 300 MHz,  $\text{D}_2\text{O}$ ): 4.14 ( $\text{CH}_2\text{CHOH}$ ), 3.45 ( $\text{CH}_2\text{CH}_2\text{OH}$ , end-group), 1.5–1.8 ( $\text{CH}_2\text{CHOH}$ ).  $M_{n,\text{NMR}} = 2140$ .

**Computational Details.** Reaction energies were calculated for a series of truncated model vanadium systems (*vide infra*) in the gas phase at 298.15 K. All calculations were performed with the Spartan 08<sup>34</sup> and Q-Chem<sup>35</sup> packages. Geometry optimizations were performed with Becke's three-parameter exchange functional (B3)<sup>36</sup> in conjunction with the correlation functional proposed by Lee, Yang, and Parr (LYP).<sup>37</sup> Vanadium atoms were modeled using the LANL2DZ effective core potential<sup>38</sup> while all other atoms were modeled using the Pople double-split-valence 6-31G\* basis set with polarization; this combination is also known as the LACVP\* hybrid basis set. Harmonic frequency calculations were performed on all optimized structures using the B3LYP/LACVP\* method to obtain thermochemical data and to confirm whether a structure corresponded to a minimum on the potential energy surface. Previous benchmark calculations on a wide range of inorganic structures including vanadium compounds indicate that such a methodology is more than adequate for our purposes.<sup>39</sup>

## RESULTS AND DISCUSSION

The pursuit of new complexes for metal-mediated controlled radical polymerization is often directed toward increasing the scope of applicable monomers within these systems. Poli and Matyjaszewski elegantly showed that certain monomers, such as vinyl acetate, are challenging to control with traditional mediators due to their higher bond dissociation energies when in the

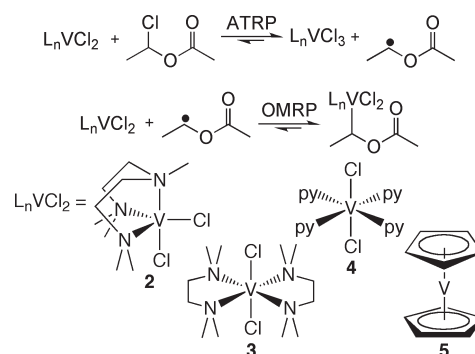


Figure 1. Vanadium(II) complexes in ATRP and OMRP equilibria.

capped form.<sup>40</sup> Poli extended this rationalization to explain the interplay between ATRP, OMRP, and reaction control in metal-mediated polymerizations.<sup>41</sup> This work suggested that the metal–carbon or metal–halogen bond strengths in copper, ruthenium, or iron systems were insufficient to balance the reactivity of more stable monomers.

Of interest to our group was whether vanadium could mediate the CRP of less reactive monomers, including vinyl acetate. Vanadium, specifically a V(II)/V(III) redox couple, was chosen due to the higher redox potentials exhibited in comparison to Cu(I)/Cu(II) systems, coupled with the precedence for V(II) complexes to homolytically cleave carbon–halogen bonds<sup>42,43</sup> and the stability of V(III) alkyl complexes.<sup>44,45</sup> While our first report in this field focused on the promise of **1**,<sup>27</sup> our initial experiments investigated whether a series of V(II) and V(III) complexes showed promise as ATRP or OMRP mediators.

Vanadium(II) complexes **2**–**5** are shown in Figure 1 and could potentially access a reversible V(II)/V(III) redox couple. Depending upon reaction conditions, these complexes could enter either an ATRP or OMRP reaction pathway. To establish an ATRP equilibrium, the complexes were reacted with 1-phenylethyl chloride to initiate the formation of radicals in the presence of 100 equiv of either styrene or vinyl acetate. The reversible homolysis of the vanadium–chlorine and carbon–chlorine bonds would establish control. Alternatively, an OMRP equilibrium may be established by combining the complex, monomer (100 equiv of styrene or vinyl acetate) and a radical source (AIBN). Thermal decomposition of the AIBN generates radicals *in situ* that may be reversibly trapped by the metal complex to control the polymer chain growth. Of these complexes,  $\text{Cp}_2\text{V}$  (**5**) was purchased and used as received,  $\text{VCl}_2(\text{py})_4$  (**4**) and  $\text{VCl}_2(\text{TMEDA})_2$  (**3**) were prepared according to reported procedures,<sup>29,30</sup> and  $[\text{PMDETA}]\text{VCl}_2$  (**2**) is a novel compound. The pentamethyldiethylenetriamine ligand (PMDETA) was chosen for two reasons. First, it has an established track record of improving performance in copper-mediated ATRP.<sup>4</sup> Second, as a tridentate ligand, it would hopefully afford a coordinatively and electronically unsaturated metal center that would readily accept additional halogen or carbon based ligands.

Complex **2** was prepared from the reaction of PMDETA with the vanadium(II) precursor  $[\text{V}_2(\mu\text{-Cl})_3(\text{THF})_6]_2[\text{Zn}_2\text{Cl}_6]$  over a 24 h period and purified by extensive washing of the resultant solid. The lilac colored complex was characterized by Evans' NMR measurements that confirmed the expected  $d^3$  electron configuration and elemental analysis. These characterization techniques are insufficient to truly define the coordination geometry and clearly do not discount the presence of a chloro-bridged dimer of **2**. Repeated



**Table 1.** ATRP and OMRP of Styrene and Vinyl Acetate Mediated by V(II) Complexes

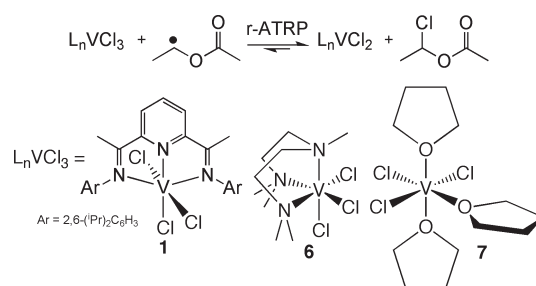
complex	monomer	conditions <sup>a,b</sup>	% conv	$M_n$	$M_{n,th}$	PDI
2	Sty	ATRP	95	61300	10035	2.55
3	Sty	ATRP	93	78800	9827	2.57
4	Sty	ATRP	98	71400	10347	2.45
5	Sty	ATRP	90	87200	9514	2.28
2	VAc	ATRP	0	n/a	n/a	n/a
3	VAc	ATRP	0	n/a	n/a	n/a
4	VAc	ATRP	0	n/a	n/a	n/a
5	VAc	ATRP	0	n/a	n/a	n/a
2	Sty	OMRP	88	32200	7933	3.15
3	Sty	OMRP	91	95200	8252	3.10
4	Sty	OMRP	85	44800	7816	3.04
5	Sty	OMRP	91	78100	8079	3.40
2	VAc	OMRP	92	22400	6895	2.65
3	VAc	OMRP	90	51900	6811	2.50
4	VAc	OMRP	95	28240	7254	2.22
5	VAc	OMRP	90	45200	6638	2.12

<sup>a</sup> ATRP polymerizations initiated with 1-PECl at 120 °C for 3 h in neat styrene or vinyl acetate with a complex:initiator:monomer ratio of 1:1:100.  $M_{n,th} = [M]_0/[I]_0 \times (\text{monomer molecular weight}) \times \% \text{ conv} + (\text{initiator molecular weight})$ . <sup>b</sup> OMRP polymerizations initiated with AIBN at 120 °C for 3 h in neat styrene or vinyl acetate with a complex:initiator:monomer ratio of 1:0.6:100.  $M_{n,th} = [M]_0/2[I]_0 \times (\text{monomer molecular weight}) \times \% \text{ conv} + (\text{catalyst molecular weight})$ .

attempts to confirm the structure by single crystal X-ray crystallography have been unsuccessful. All vanadium(II) complexes were highly air-sensitive and were handled under N<sub>2</sub>, prepared fresh, and purified by recrystallization prior to use. Attempts to synthesize a vanadium(II) complex supported by the aforementioned BIMPY ligand have thus far been unsuccessful.

Data for screening reactions of complexes 2–5 with styrene and vinyl acetate under both ATRP and OMRP conditions are shown in Table 1. While these mediators do not control these polymerizations, there are clear trends that support the principle of these systems. Under ATRP conditions styrene polymerizations are uncontrolled because the radical concentrations are too high. The strong V–Cl bond favors uncapped chains and leads to high molecular weights and broad polydispersities. Under ATRP conditions vinyl acetate polymerizations show no productive polymer formation. The capped form is favored, and radical concentrations are too low to produce poly(vinyl acetate). Under OMRP conditions both styrene and vinyl acetate polymerizations are uncontrolled due to inefficient trapping of the propagating radical chains by the metal complex. For each catalytic system, however, the vinyl acetate monomer shows lower molecular weights at equivalent conversions and more narrow polydispersities, suggesting some measure of control over the polymerization reactions. This correlates well with the expected increase in strength between the two vanadium–carbon bonds.

Vanadium(III) complexes are usually more stable and more readily characterized than their V(II) congeners. These species can engage in a reverse ATRP equilibrium whereby initiated and growing radicals can reversibly abstract a halogen from the complex. The same reaction conditions could conceivably establish a formally V(III)/V(IV) OMRP-type equilibrium with the reversible formation of a metal–carbon bond. Complexes 1, 6,

**Figure 2.** Vanadium(III) complexes used in reverse ATRP protocols.**Table 2.** Reverse ATRP Conditions for Styrene and Vinyl Acetate Polymerization Mediated by V(III) Complexes

complex	monomer	conditions <sup>a</sup>	% conv	$M_n$	$M_{n,th}^b$	$M_{n,th}^c$	PDI
1	Sty	r-ATRP	45	12413	3906	7811	2.25
6	Sty	r-ATRP	80	87572	6943	13887	2.51
7	Sty	r-ATRP	62	90480	5381	10762	2.50
1	VAc	r-ATRP	31	4490	2224	4448	1.26
6	VAc	r-ATRP	57	36338	4089	8179	1.41
7	VAc	r-ATRP	68	20342	4878	9757	1.63

<sup>a</sup> Polymerizations initiated with AIBN at 120 °C for 4 h in neat styrene or vinyl acetate with a complex:initiator:monomer ratio of 1:0.6:100.

<sup>b</sup>  $M_{n,th} = [M]_0/2[I]_0 \times (\text{monomer molecular weight}) \times \% \text{ conv}$ .

<sup>c</sup>  $M_{n,th} = [M]_0/[I]_0 \times (\text{monomer molecular weight}) \times \% \text{ conv}$ .

and 7 were screened for the AIBN-initiated CRP of styrene and vinyl acetate. The complexes and reaction equation are shown in Figure 2 along with tabulated data in Table 2.

In the radical polymerization of vinyl acetate it is clear that all of the V(III) catalysts offer some modicum of control, consistently showing lowered polydispersities and molecular weights than either V(II)-mediated vinyl acetate polymerizations or V(III)-mediated styrene polymerizations. In particular, complex 1 offers excellent control over both molecular weights and polydispersity. This V(III) bis(imino)pyridine complex was first reported as an active catalyst for the oligomerization and polymerization of ethylene<sup>31,46</sup> and butadiene<sup>47</sup> and the dimerization of propylene.<sup>48</sup> The noninnocence of the BIMPY ligand set is also well documented for vanadium in the decomposition of polymerization catalysts,<sup>46</sup> the activation of molecular nitrogen,<sup>49</sup> and, in a more formal sense, the electrochemical characterization of M(BIMPY)<sub>2</sub> cations.<sup>50</sup>

We investigated the CRP of vinyl acetate by 1. Kinetic studies confirmed that the process was first order in monomer, as exhibited by the linear dependence of  $\ln([M]_0/[M])$  versus time at three different temperatures (Supporting Information Figure S1). Effective control was only achieved at 120 °C due to the inefficient initiation of AIBN at lower temperatures (Figure S2). The polymerization reaction was controlled at these elevated temperatures, as indicated by a linear correlation between polymer molecular weights and % monomer conversion. A standard calculation of expected molecular weights (200 monomers/chain  $\times$  86.09 g/mol  $\times$  % conversion) shows that observed molecular weights are consistently higher by ~650 g/mol (Figure 3, dashed line). Recognition that the vanadium complex (639 g/mol) could be acting as the end-group for this polymerization gave expected molecular weights that correlated remarkably well with those observed (Figure 3,

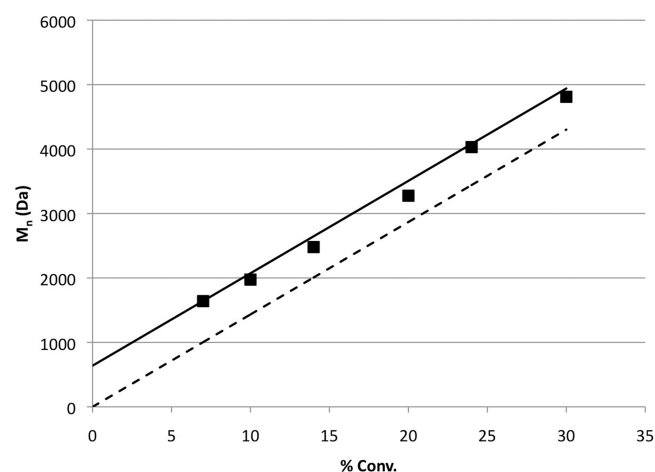
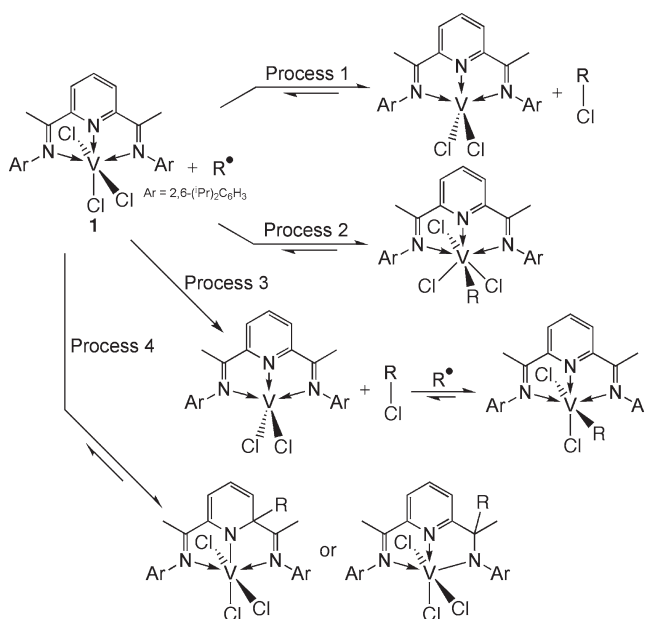


**Figure 3.** Dependence of poly(vinyl acetate)  $M_n$  on monomer conversion for the bulk polymerization of vinyl acetate at 120 °C.

solid line), indicating that the metal-capped chains do not possess significantly different hydrodynamic volumes to proton-terminated poly(vinyl acetate) chains. Isolating polymers at moderate to high conversions was challenging due to complex decomposition. High conversion polymerizations were inconsistent, either deviating significantly from expected values or resulting in nonproductive polymerizations. Decomposition of **1** under reaction conditions occurs after ca. 6 h at 120 °C, while decomposition in the absence of radicals is negligible even after 24 h at 120 °C. Within the first 6 h of reaction time, however, the polymerization is well controlled. Start–stop experiments (Figure S3), both by cooling the reaction medium to –30 °C for 24 h and reheating to 120 °C and through isolating the polymer by precipitation and restarting with a second aliquot of monomer, indicate living characteristics. The vanadium terminus of the polymer chain could be readily removed by either addition of propanethiol to generate proton-terminated PVAc or base-catalyzed methanolysis to generate proton-terminated poly(vinyl alcohol) chains.

While investigating this reaction further, it quickly became apparent that there were a number of mechanistic possibilities for this process (Scheme 1). The poly(vinyl acetate), PVAc, generated from this reaction was dark red-brown in color but readily soluble in polar organic solvents. Analysis of the material by NMR spectroscopy suggested that, while control was achieved, it was unlikely that an ATRP equilibrium was established (process 1). No halogen-capped polymer chains were observed, and 1D and 2D spectra showed a washing-out and broadening of resonances. Small, broadened resonances attributable to paramagnetically shifted BIMPY ligand resonances were observed but were too broad to definitively assign. Coupled with the color of the polymeric material even after purification, this suggested that an OMRP equilibrium was playing a role and that the dormant polymer was a vanadium organometallic, a statement further supported by XPS and EPR data on the polymer confirming the presence of vanadium (Figures S6 and S7). A formally V(III)/V(IV) equilibrium does not mesh with a basic understanding of vanadium coordination chemistry as it would require a seven-coordinate vanadium organometallic, [BIMPY]VCl<sub>3</sub>R, that would need to be thermodynamically favored over the [BIMPY]VCl<sub>3</sub> parent complex to significantly lower radical concentrations (process 2). Two other possibilities also exist: the

**Scheme 1.** Potential Controlled Radical Polymerization Pathways for [BIMPY]VCl<sub>3</sub>



irreversible abstraction of a chlorine by initiating radicals would *in situ* generate a V(II) intermediate that could reversibly trap the growing free radicals by an OMRP equilibrium (process 3) while reversible carbon–carbon bond formation could occur through combination of the growing free radical with a ligand-based radical (process 4). Process 4 in particular recognizes that the noninnocent ligand can play a significant role in this reaction and builds upon previous reports of MeLi reacting with [BIMPY]VCl<sub>3</sub> to methylate the ortho position of the pyridyl ring.<sup>46</sup> It should also be recognized that multiple mechanisms may be in operation at once.

Our initial communication of this work<sup>27</sup> also presented early mechanistic investigations that supported process 3. This evidence included corrected molecular weights that were double those expected if an AIBN molecule decomposed into two propagating radicals, suggesting that  $[R^\bullet] = \frac{1}{2}[AIBN]$ . This is expected if the  $(CH_3)_2(CN)C^\bullet$  or growing polymer radical dechlorinates the [BIMPY]VCl<sub>3</sub> catalyst to generate  $(CH_3)_2(CN)CCl$ , **8**, and the active complex. If the propagating radicals react preferentially with the V(II) species and are less halogenophilic, the OMRP equilibrium would be established and expected molecular weights would be effectively doubled. Further support was found in the identification of small quantities of **8** in gas chromatographic analysis of the monomer feed in an early stage polymerization. Quantification of this peak suggests significantly less than 1 equiv of **8** is formed, limiting the conclusiveness of this finding. It might be expected that halogen-terminated, short-chain oligomeric species could also form, reducing the observed quantity of **8**, but species such as  $(CH_3)_2(CN)C(VAc)_nCl$  could not be identified in the gas chromatographic traces. In addition, alkylation of the BIMPY backbone with MeLi<sup>46</sup> creates a complex which inhibits rather than initiates vinyl acetate polymerization, suggesting the backbone alkylation may be irreversible. With so many important mechanistic questions remaining unanswered, further investigation of this system both experimentally and computationally was warranted.

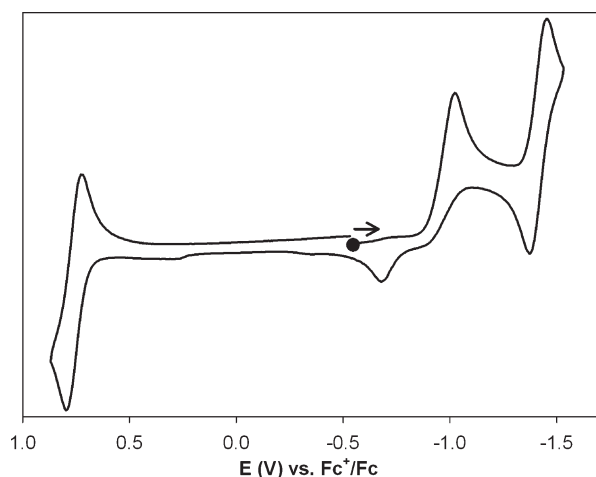


**Figure 4.** Cyclic voltammogram (vs  $\text{Fc}^+/\text{Fc}$ ) of **1**. Conditions: 5 mM complex, 0.1 M  $\text{NBu}_4\text{ClO}_4$ , scan rate 100 mV/s,  $\text{CH}_3\text{CN}$ , 230 K.

**Table 3.** Redox Potentials for **1** vs  $\text{Fc}^+/\text{Fc}$ <sup>a</sup> at 230 K;<sup>a</sup> Peak-to-Peak Differences in Parentheses ( $|E_{\text{pc}} - E_{\text{pa}}|$ )<sup>b</sup>

$[\text{I}]^+/\text{I}$ (V)	$\text{I}/[\text{I}]^-$ (V)	$[\text{I}]^-/[\text{I}]^{2-}$ (V)
0.78 (0.175)	$E_{\text{anodic}}: -1.02$ $E_{\text{cathodic}}: -0.65$	-1.40 (0.171)

<sup>a</sup> 5 mM complex, 0.1 M  $\text{NBu}_4\text{ClO}_4$ , scan rate 100 mV/s,  $\text{CH}_3\text{CN}$ , 230 K.

<sup>b</sup> Peak-to-peak difference for the  $\text{Fc}^+/\text{Fc}$  couple at 230 K is 0.189 V.

**Electrochemical Studies of [BIMPY]VCl<sub>3</sub>.** Cyclic voltammetry (CV) experiments were used to probe the redox processes for **1**. The CV spectrum of **1** was recorded in  $\text{CH}_3\text{CN}$  solution containing 0.10 M  $\text{NBu}_4\text{ClO}_4$  as the supporting electrolyte (Figure 4). Ferrocene was used as the internal standard, and potentials are referenced vs the ferrocenium/ferrocene ( $\text{Fc}^+/\text{Fc}$ ) couple (Table 3). Two one-electron redox processes are observed at negative potentials, with a further one-electron redox couple present at positive potential. The reversibility of the redox couple at 0.78 V is improved at low temperature, and so the experiment was completed at 230 K. The reversible couple at positive potential is assigned as a metal-based  $\text{V}^{\text{III}}/\text{V}^{\text{IV}}$  couple, as ligand oxidative processes are not accessible in the electrochemical window.<sup>50</sup> The reversible redox process at -1.40 V is much more difficult to assign (ligand vs metal) due to the documented noninnocence of the bis(imino)pyridine ligand framework.<sup>49–52</sup> The first reduction process is irreversible under the experimental conditions, and no significant changes to the CV spectrum were observed when using either  $\text{CH}_2\text{Cl}_2$  as the solvent or  $\text{NBu}_4\text{PF}_6$  as the supporting electrolyte. Interestingly, the CV curve of the first reduction process does not change with repetitive scanning (Figure S8). This result suggests that the irreversible redox process does not lead to chemical decomposition of the complex and could be a result of substantial reorganization energy of the reduced or oxidized complex.<sup>53</sup> While ligand ( $\text{L} \rightarrow \text{L}^{\cdot-}$ ) or metal reduction ( $\text{V}^{\text{III}} \rightarrow \text{V}^{\text{II}}$ ) could account for significant geometrical changes, we favor the former on the basis of the computational studies (*vide infra*) and reversible ligand reduction processes reported for other transition metal complexes of bis(imino)pyridine ligands.<sup>50</sup> The change in electronic structure upon reduction is likely accompanied by a structural change to form the ligand radical. We cannot discount that chlorine ion loss is

**Table 4.** Summary of Overall Gas-Phase Reaction Enthalpies, Entropies (at 298 K), and Free Energies for Each Process in Scheme 1<sup>a</sup>

reaction <sup>b</sup>	$\Delta H$	$T\Delta S$	$\Delta G$
process 1 (Sty)	-13.20	-0.30	-12.90
process 2 (Sty)	n/a	n/a	n/a
process 3a (Sty)	-13.20	-0.30	-12.90
process 3b (Sty, a)	5.07	-14.87	19.93
process 3b (Sty, e)	6.27	-15.32	21.59
process 4 (Sty, py, R)	14.32	-14.26	28.58
process 4 (Sty, py, S)	15.22	-14.70	29.92
process 4 (Sty, im, R)	-9.49	-15.88	6.40
process 4 (Sty, im, S)	-11.96	-15.95	3.99
process 1 (VAc)	-23.95	0.16	-24.11
process 2 (VAc)	n/a	n/a	n/a
process 3a (VAc)	-23.95	0.16	-24.11
process 3b (VAc, a)	-6.51	-14.60	8.09
process 3b (VAc, e)	-11.57	-15.47	3.91
process 4 (VAc, py, R)	4.23	-14.19	18.42
process 4 (VAc, py, S)	-0.20	-14.56	14.36
process 4 (VAc, im, R)	-22.33	-15.16	-7.16
process 4 (VAc, im, S)	-23.95	-14.96	-8.99

<sup>a</sup> All values in kcal/mol. <sup>b</sup> Sty = styrene, VAc = vinyl acetate, a = axial coordination, e = equatorial coordination, R/S = enantiomer formed upon radical addition, py = attack at pyridine carbon, im = attack at imine carbon.

occurring upon reduction, but the current CV results suggest that the reversible redox process does not lead to decomposition of the complex on the CV time scale.

**Computational Investigation of Mechanism.** Processes 1–4 were also investigated computationally using the truncated ligand system <sup>Me</sup>[BIMPY], where <sup>Me</sup>[BIMPY] = 2,6-(MeN=CH)<sub>2</sub>-(C<sub>5</sub>H<sub>3</sub>N), supporting the various vanadium complexes and  $[\text{CH}_3\text{CHPh}]^{\cdot}$  (Sty<sup>•</sup>) or  $[\text{CH}_3\text{CHOCOCH}_3]^{\cdot}$  (VAc<sup>•</sup>) radicals. Comparing the enthalpies, entropies, and free energies of the reactant and product species for each process affords valuable insight into the viability of each potential reaction pathway.

The overall thermochemistry calculated for the complexes is provided in Table 4, and a reaction coordinate diagram for the various mechanistic possibilities is shown in Figures 5 and 6. Both the R and S products resulting from Sty<sup>•</sup> or VAc<sup>•</sup> addition were calculated as slight differences in energies were noted due to differences in steric interactions between the two potential products.

Process 1, formally establishing an ATRP equilibrium, is thermodynamically favored by ~24 kcal/mol with VAc<sup>•</sup>, suggesting it is unlikely that this dehalogenation step is reversible. The favorability of this step is significantly lower for Sty<sup>•</sup> (-13 kcal/mol), predominantly due to the stability of the free radical. Regardless of monomer, it would not be feasible for a reversible halogen transfer to facilitate the controlled radical polymerization. Process 2, involving the trapping of an alkyl radical by the parent <sup>Me</sup>[BIMPY]VCl<sub>3</sub> complex, is unlikely to occur. All attempts to optimize a thermodynamically stable structure failed, and in each case the optimization proceeded to remove the radical from the vanadium center, indicating that the already crowded metal could not accommodate yet another substituent. The <sup>Me</sup>[BIMPY]VCl<sub>3</sub>R species is thus not predicted to exist, and as expected, process 2 is not thermodynamically viable.

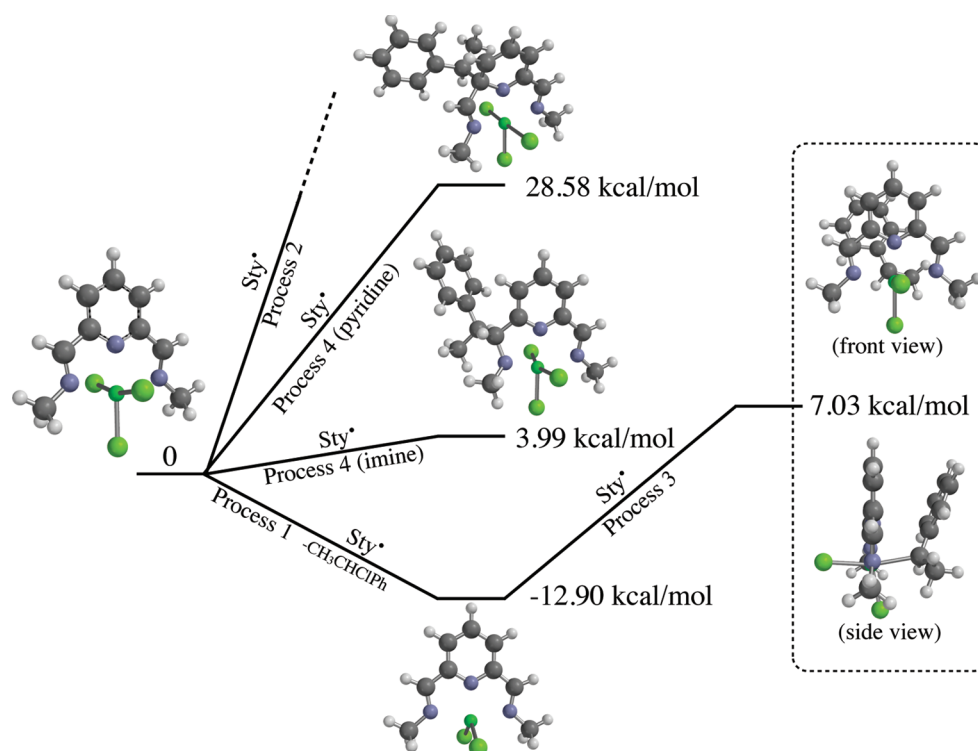


**Figure 5.** Reaction coordinate diagram,  $\Delta G$  values, and optimized structures of processes 1–4 involving the styrene radical.

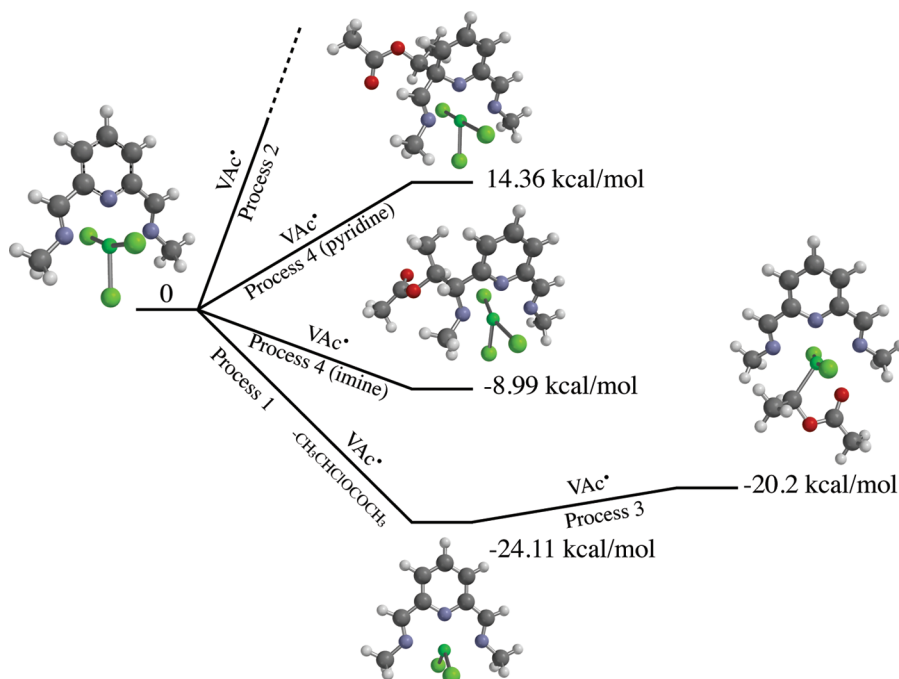


**Figure 6.** Reaction coordinate diagram,  $\Delta G$  values, and optimized structures of processes 1–4 involving the vinyl acetate radical.

Process 4 was investigated by targeting two potential alkylation sites on the bis(imino)pyridine framework representing attack at the electrophilic pyridyl and imine carbons, respectively. Early synthetic work by Gambarotta et al. with  $i\text{Pr}^{\text{Ph}}[\text{BIMPY}]\text{-VCl}_3$  and MeLi suggested that the pyridyl carbon was more susceptible to nucleophilic attack.<sup>46</sup> In the presence of carbon-

based radicals, however, attack at the imine carbon of  $\text{Me}[\text{BIMPY}]\text{VCl}_3$  is significantly more favorable (by  $\sim 20$  kcal/mol), regardless of radical choice. This overall reaction is thermodynamically unfavorable for styrenyl radicals but favored slightly for vinyl acetate species, again suggesting that monomer stability plays a key role in reaction energetics.



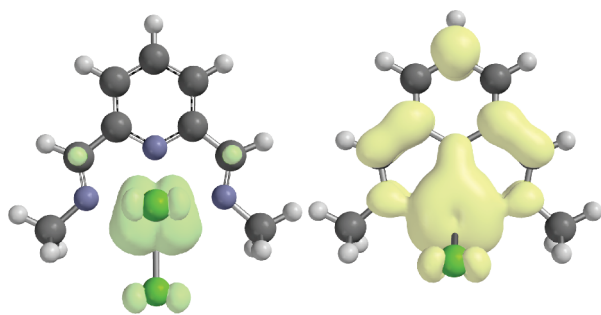


**Figure 7.** Isosurface plots of the B3LYP/LCAVP\* spin densities for the  $^{\text{Me}}[\text{BIMPY}]\text{VCl}_3$  (left) and  $^{\text{Me}}[\text{BIMPY}]\text{VCl}_2$  (right) systems ( $\rho = 0.002$  au).

This theoretical study clearly supports process 3 as a viable option to control the radical polymerization of vinyl acetate. A small differential of 4 kcal/mol separates the parent  $^{\text{Me}}[\text{BIMPY}]\text{VCl}_2$  complex and the  $^{\text{Me}}[\text{BIMPY}]\text{VCl}_2(\text{VAc})$  organometallic, suggesting that this process may be reversible. While the energy implies that the radical trapping step would be endothermic, it is well within the accuracy limits of this computational study and may change when investigating a nontruncated ligand set or solvent effects are included. Interestingly, this computational study also supports the disparity in control over styrene and vinyl acetate polymerizations, as the  $^{\text{Me}}[\text{BIMPY}]\text{VCl}_2 + \text{Sty}^\bullet$  reaction is endergonic by 20 kcal/mol. Comparing the Sty and VAc stationary structures provides a reasoning for this differentiation (Figures 5 and 6). Participation of the ester carbonyl group in chelating to the metal center stabilizes the trapped vinyl acetate species and makes V–C bond formation nearly thermodynamically neutral. Chelation of this carbonyl group to the metal center has been previously reported for calculations on the  $\text{Co}(\text{acac})_2$  system, with a six-coordinate dormant species proposed.<sup>12</sup>

Examination of the spin densities of the key  $^{\text{Me}}[\text{BIMPY}]\text{VCl}_3$  and  $^{\text{Me}}[\text{BIMPY}]\text{VCl}_2$  complexes indicates that ligand noninnocence may play an important role in this reaction. Figure 7 illustrates that while the unpaired electrons in the starting trichloride are localized on the metal, the spin density is spread throughout the ligand backbone in the reduced dichloride intermediate. The increase in spin density on the  $^{\text{Me}}[\text{BIMPY}]$  ligand in the reduced system may correlate to the geometrical reorganization expected to occur after electrochemical reduction experiments (*vide supra*)<sup>54</sup> and supports the characterization of this  $[\text{BIMPY}]\text{VCl}_2$  species as a V(III) ligand radical.

These results demonstrate that this vanadium catalyst operates through a unique, two-step reaction pathway: dehalogenation to form a reactive V(II) intermediate and reversible OMRP to control the polymerization of vinyl acetate. Control over vinyl acetate is facilitated by both the higher reactivity of the radical species and the participation of the ester group in the trapping step.

**Extension of the Vanadium-Based OMRP Reaction.** In an effort to gauge the utility of **1** in CRP, we extended our initial reactivity studies in a number of directions. Even with short catalyst lifetimes, higher molecular weight PVAc is accessible by altering the monomer: initiator ratios. Figure 8 details a kinetic study of the growth of polymer chains using 1:AIBN:VAc ratios of 1:0.6:300 and 1:0.6:500. A linear increase in  $M_n$  with conversion and moderate PDIs of 1.28–1.38 suggest control is maintained up to  $M_n = 10\,200$  and  $15\,600$  Da, respectively, correlating

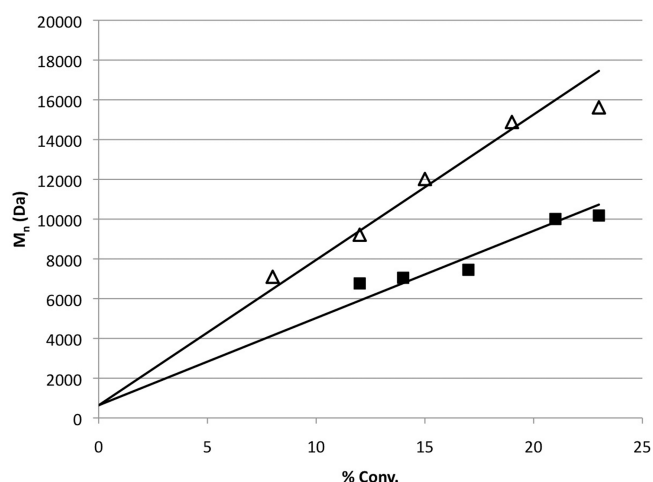


**Figure 8.** Dependence of poly(vinyl acetate)  $M_n$  on monomer conversion for the bulk polymerization of vinyl acetate at  $120^\circ\text{C}$  with 1:AIBN:VAc ratios of 1:0.6:300 (■) and 1:0.6:500 (Δ).

to 23% conversion in each case. After 6 h, catalyst degradation results in a loss of control and no further monomer conversion, which suggests that catalyst death is not dependent on the monomer concentration.

Further effort was placed on investigating the scope of this vanadium-based OMRP system. Our initial report focused on the polymerization of vinyl acetate and styrene. Styrene, in particular, presents intriguing features. The computations suggest that the radical trapping reaction is more thermodynamically stable for vinyl acetate than styrene, agreeing with polymerization results. However, elements of control remain. While it is clear that the early stages of the reaction are uncontrolled, a modicum of control is achieved after 10–20% conversion (Figure S4), supported by linear kinetics of monomer consumption (Figure S5). Polydispersities increase to  $\sim 1.6$  in the early stages of this polymerization but do not rise significantly from this point. These results suggest that tuning the ligand and refining the initiation process are key requirements for expanding the monomer scope, and these are areas of current research for our team.

Table 5 communicates further monomer screening conducted with **1** under OMRP conditions. As expected, polymerization of the reactive monomers methyl methacrylate (MMA) and acrylonitrile (AN) are uncontrolled, giving high molecular weight polymers with broad polydispersities, in agreement with the aforementioned monomer reactivity trends.<sup>40</sup> Vinyl ester monomers show more promise. At  $120^\circ\text{C}$ , vinyl propionate (VPr) and vinyl pivalate (VPv) monomers exhibit good control with polydispersities of 1.35 and 1.36, respectively. Vinyl benzoate (VBz) is less controlled, with a broadened PDI of 1.56. Molecular weights are corrected with vinyl acetate parameters, so some deviation between determined and theoretical molecular weights is expected, and observed, due to differences in hydrodynamic volumes between monomers. Conversions are again low due to catalyst death; no productive polymerization occurs after 6 h. At lower temperatures this decomposition is mitigated somewhat and higher conversions are observed, providing access to moderately high molecular weight poly(vinyl esters). Control over these polymerizations is likely to be facilitated by the participation of the ester carbonyl group in the trapping step, analogous to the minimized structures observed for vinyl acetate vanadium complexes.

**Table 5.** OMRP of Methyl Methacrylate, Acrylonitrile, Vinyl Propionate, Vinyl Pivalate, and Vinyl Benzoate with **1**

monomer <sup>a</sup>	temp (°C)	time (h)	% conv	$M_n$	$M_{n,th}$	PDI
MMA	120	1.0	88	28567	9369	2.15
AN	120	1.5	71	114000	4218	2.89
VPr	120	6.0	20	3529	3990	1.35
VPv	120	6.0	36	9344	8316	1.36
VBz	120	6.0	20	3955	5615	1.56
VPr	90	6.0	30	5618	5666	1.35
VPv	90	6.0	53	15009	11942	1.37
VBz	90	6.0	19	3762	5366	1.57

<sup>a</sup> Bulk polymerizations initiated with AIBN at 120 °C, with a complex: initiator:monomer ratio of 1:0.6:100.  $M_{n,th} = [M]_0/[I]_0 \times (\text{monomer molecular weight}) \times \% \text{ conv} + (\text{catalyst molecular weight})$ .

Our current research is focused principally on catalyst design to access more thermally robust vanadium complexes in an effort to prevent complex decomposition and access higher monomer conversions. Efforts to use OMRP to prepare block copolymers of multiple vinyl esters and telechelic poly(vinyl acetate)s are also underway and will be the focus of a future report.

## CONCLUSIONS

Given the limited range of transition metal systems currently available for OMRP, expansion to vanadium is an exciting development. A range of V(II) and V(III) complexes have been investigated for the controlled radical polymerization of styrene and vinyl acetate. Isolated V(II) species are inefficient mediators, under both ATRP and OMRP conditions. However, while V(III) complexes are unable to control polymerization through an ATRP regime, they exert reasonable control (PDIs 1.3–1.6) over vinyl acetate polymerization when initiated by AIBN. In particular, [BIMPY]VCl<sub>3</sub> provides excellent control over the polymerization of vinyl acetate. The reactions are first order in monomer, with molecular weights which increase linearly with conversion, correlating well with theoretical values, and PDIs of <1.3. Mechanistic studies, both experimental and computational, reveal that control is derived solely from the OMRP regime, with dehalogenation of the parent V(III) complex forming the active [BIMPY]VCl<sub>2</sub> *in situ*. This species acts as a persistent radical, trapping the propagating radical chains and establishing the OMRP equilibrium. Control over vinyl acetate is derived both from the higher reactivity of the VAc<sup>•</sup> radical and participation of the carbonyl oxygen of the ester group in the trapping step. Although more reactive monomers such as methyl methacrylate, acrylonitrile, and styrene are poorly controlled by this system, it is also active for other vinyl esters, with unoptimized screening reactions showing good control over molecular weights and reasonable PDIs.

## ASSOCIATED CONTENT

**S Supporting Information.** Additional polymerization and characterization data and molecular modeling coordinates. This material is available free of charge via the Internet at <http://pubs.acs.org>.

## AUTHOR INFORMATION

### Corresponding Author

\*E-mail: [mshaver@upei.ca](mailto:mshaver@upei.ca).

## ACKNOWLEDGMENT

The authors thank the Natural Sciences and Engineering Research Council of Canada (MS and TS), the Canada Foundation for Innovation (MS), the Atlantic Canada Opportunities Agency (MS), and the University of Prince Edward Island (MS and JP) for funding.

## REFERENCES

- (1) Hawker, C. J.; Bosman, A. W.; Harth, E. *Chem. Rev.* **2001**, *101*, 3661–3688.
- (2) Moad, G.; Rizzardo, E.; Thang, S. H. *Acc. Chem. Res.* **2008**, *41*, 1133–1142.
- (3) Moad, G.; Rizzardo, E.; Thang, S. H. *Aust. J. Chem.* **2005**, *58*, 379–410.
- (4) Matyjaszewski, K.; Xia, J. *Chem. Rev.* **2001**, *101*, 2921–2990.
- (5) Ouchi, M.; Terashima, T.; Sawamoto, M. *Acc. Chem. Res.* **2008**, *41*, 1120–1132.
- (6) di Lena, F.; Matyjaszewski, K. *Prog. Polym. Sci.* **2010**, *35*, 959–1021.
- (7) Poli, R. *Eur. J. Inorg. Chem.* **2011**, *2011*, 1513–1530.
- (8) Smith, K. M.; McNeil, W. S.; Abd-El-Aziz, A. S. *Macromol. Chem. Phys.* **2010**, *211*, 10–16.
- (9) Wayland, B. B.; Poszmik, G.; Mukerjee, S. L.; Fryd, M. J. *Am. Chem. Soc.* **1994**, *116*, 7943–7944.
- (10) Debuigne, A.; Caille, J. R.; Jérôme, R. *Angew. Chem., Int. Ed.* **2005**, *44*, 1101–1104.
- (11) Maria, S.; Kaneyoshi, H.; Matyjaszewski, K.; Poli, R. *Chem.—Eur. J.* **2007**, *13*, 2480–2492.
- (12) Debuigne, A.; Champouret, Y.; Jérôme, R.; Poli, R.; Detrembleur, C. *Chem.—Eur. J.* **2008**, *14*, 4046–4059.
- (13) Debuigne, A.; Poli, R.; Jérôme, R.; Jérôme, C.; Detrembleur, C. *ACS Symp. Ser.* **2009**, *1024*, 131–147.
- (14) Le Grogne, E.; Claverie, J.; Poli, R. *J. Am. Chem. Soc.* **2001**, *123*, 9513–9524.
- (15) Stoffelbach, F.; Poli, R.; Richard, P. *J. Organomet. Chem.* **2002**, *663*, 269–276.
- (16) Maria, S.; Stoffelbach, F.; Mata, J.; Daran, J.-C.; Richard, P.; Poli, R. *J. Am. Chem. Soc.* **2005**, *127*, 5946–5956.
- (17) Braunecker, W. A.; Itami, Y.; Matyjaszewski, K. *Macromolecules* **2005**, *38*, 9402–9404.
- (18) Shaver, M. P.; Allan, L. E. N.; Rzepa, H. S.; Gibson, V. C. *Angew. Chem., Int. Ed.* **2006**, *45*, 1241–1244.
- (19) Shaver, M. P.; Allan, L. E. N.; Gibson, V. C. *Organometallics* **2007**, *26*, 4725–4730.
- (20) Champouret, Y.; Baisch, U.; Poli, R.; Tang, L.; Conway, J.; Smith, K. *Angew. Chem., Int. Ed.* **2008**, *47*, 6069–6072.
- (21) Champouret, Y.; MacLeod, K. C.; Baisch, U.; Patrick, B. O.; Smith, K. M.; Poli, R. *Organometallics* **2010**, *29*, 167–176.
- (22) Champouret, Y.; MacLeod, K. C.; Smith, K. M.; Patrick, B. O.; Poli, R. *Organometallics* **2010**, *29*, 3125–3132.
- (23) Destarac, M.; Charmot, D.; Franck, X.; Zard, S. Z. *Macromol. Rapid Commun.* **2000**, *21*, 1035–1039.
- (24) Rizzardo, E.; Chiefari, J.; Mayadunne, R.; Moad, G.; Thang, S. *Macromol. Symp.* **2001**, *174*, 209–212.
- (25) Stenzel, M. H.; Cummins, L.; Roberts, G. E.; Davis, T. P.; Vana, P.; Barner-Kowollik, C. *Macromol. Chem. Phys.* **2003**, *204*, 1160–1168.
- (26) Debuigne, A.; Poli, R.; Jérôme, C.; Jérôme, R.; Detrembleur, C. *Prog. Polym. Sci.* **2009**, *34*, 211–239.
- (27) Shaver, M. P.; Hanhan, M. E.; Jones, M. R. *Chem. Commun.* **2010**, *46*, 2127–2129.
- (28) Manzer, L. E. *Inorg. Synth.* **1982**, *21*, 135–140.
- (29) Khamar, M.; Larkworthy, L.; Patel, K.; Phillips, D.; Beech, G. *Aust. J. Chem.* **1974**, *27*, 41–51.
- (30) Edema, J. J. H.; Stauffer, W.; Van Bolhuis, F.; Gambarotta, S.; Smeets, W. J. J.; Spek, A. L. *Inorg. Chem.* **1990**, *29*, 1302–1306.

- (31) Milione, S.; Cavallo, G.; Tedesco, C.; Grassi, A. *J. Chem. Soc., Dalton Trans.* **2002**, 1839–1846.
- (32) Romero, J.; Carrillo-Hermosilla, F.; Antinolo, A.; Otero, A. *J. Mol. Catal. A: Chem.* **2009**, 304, 180–186.
- (33) Gruending, T.; Junkers, T.; Guilhaus, M.; Barner-Kowollik, C. *Macromol. Chem. Phys.* **2010**, 211, 520–528.
- (34) Spartan '08, Wavefunction Inc., Irvine, CA.
- (35) Shao, Y.; *Phys. Chem. Chem. Phys.* **2006**, 8, 3172–3191.
- (36) Becke, A. D. *J. Chem. Phys.* **1993**, 98, 5648–5652.
- (37) Lee, C.; Yang, W.; Parr, R. G. *Phys. Rev. B: Condens. Matter* **1988**, 37, 785–789.
- (38) Hay, P. J.; Wadt, W. R. *J. Chem. Phys.* **1985**, 82, 299–310.
- (39) Bytheway, L.; Wong, M. W. *Chem. Phys. Lett.* **1998**, 282, 219–226.
- (40) Gillies, M. B.; Matyjaszewski, K.; Norrby, P.-O.; Pintauer, T.; Poli, R.; Richard, P. *Macromolecules* **2003**, 36, 8551–8559.
- (41) Poli, R. *Angew. Chem., Int. Ed.* **2006**, 45, 5058–5070.
- (42) Cooper, T. A. *J. Am. Chem. Soc.* **1973**, 95, 4158–4162.
- (43) Cooper, T. A.; Sonnenberg, F. M. *J. Org. Chem.* **1975**, 40, 55–57.
- (44) Espenson, J. H.; Bakac, A.; Kim, J. H. *Inorg. Chem.* **1991**, 30, 4830–4833.
- (45) Brussee, E. A. C.; Meetsma, A.; Hessen, B.; Teuben, J. H. *Organometallics* **1998**, 17, 4090–4095.
- (46) Reardon, D.; Conan, F.; Gambarotta, S.; Yap, G.; Wang, Q. *J. Am. Chem. Soc.* **1999**, 121, 9318–9325.
- (47) Colamarco, E.; Milione, S.; Cuomo, C.; Grassi, A. *Macromol. Rapid Commun.* **2004**, 25, 450–454.
- (48) Lang, J. R. V.; Denner, C. E.; Alt, H. G. *J. Mol. Catal. A: Chem.* **2010**, 322, 45–49.
- (49) Vidyaratne, I.; Gambarotta, S.; Korobkov, I.; Budzelaar, P. H. M. *Inorg. Chem.* **2005**, 44, 1187–1189.
- (50) de Bruin, B.; Bill, E.; Bothe, E.; Weyhermüller, T.; Wieghardt, K. *Inorg. Chem.* **2000**, 39, 2936–2947.
- (51) Bart, S. C.; Chłopek, K.; Bill, E.; Bouwkamp, M. W.; Lobkovsky, E.; Neese, F.; Wieghardt, K.; Chirik, P. J. *J. Am. Chem. Soc.* **2006**, 128, 13901–13912.
- (52) Manuel, T. D.; Rohde, J.-U. *J. Am. Chem. Soc.* **2009**, 131, 15582–15583.
- (53) Bard, A. J.; Faulkner, L. R. *Electrochemical Methods, Fundamentals and Applications*; John Wiley & Sons: New York, 1980; Chapters 6 and 11.
- (54) A calculation on the reduced trichloride complex also predicts increased spin density on the ligand backbone, matching the result for Me[BIMPY]VCl<sub>2</sub>.